Using Flux by Cloud Type Data to Study Convective Aggregation in the Tropics

Kuan-Man Xu[1], Yaping Zhou[2], Moguo Sun[3], Seiji Kato[1], Yong Hu[1]

1. NASA Langley Research Center, Hampton, VA
2. University of Maryland-Baltimore County/GSFC
3. Analytical Mechanics Associates, Inc./Langley Research Center

Xu *et al.* (2023): Observed cloud type-sorted cloud property and radiative flux changes with the degree of convective aggregation from CERES data. *J. Geophys. Res., 128, https://doi.org/10.1029/2023JD039152.*

What is convective self-aggregation (CSA)? Cloud-resolving model (CRM) example

- A self-aggregation phenomenon in idealized radiative-convective equilibrium simulations under constant, uniform SST;
- Mechanism: feedbacks among convection, moisture, clouds, radiation & surface fluxes;
- Radiative feedbacks are particularly important in addition to moisture feedbacks;
- For onset, the longwave cooling near the top of low clouds in dry and subsiding regions forces a shallow circulation that induces upgradient energy transports and radiative-convective instability;
- The strong clear-sky radiative cooling in the dry region and heating in the cloudy regions due to high clouds play a major role in maintaining the CSA (& deep circulation);
- Shortwave radiative heating and cool pools tend to weaken CSA while surface fluxes tend to strengthen CSA at the initial stage but weaken CSA at the later stage.

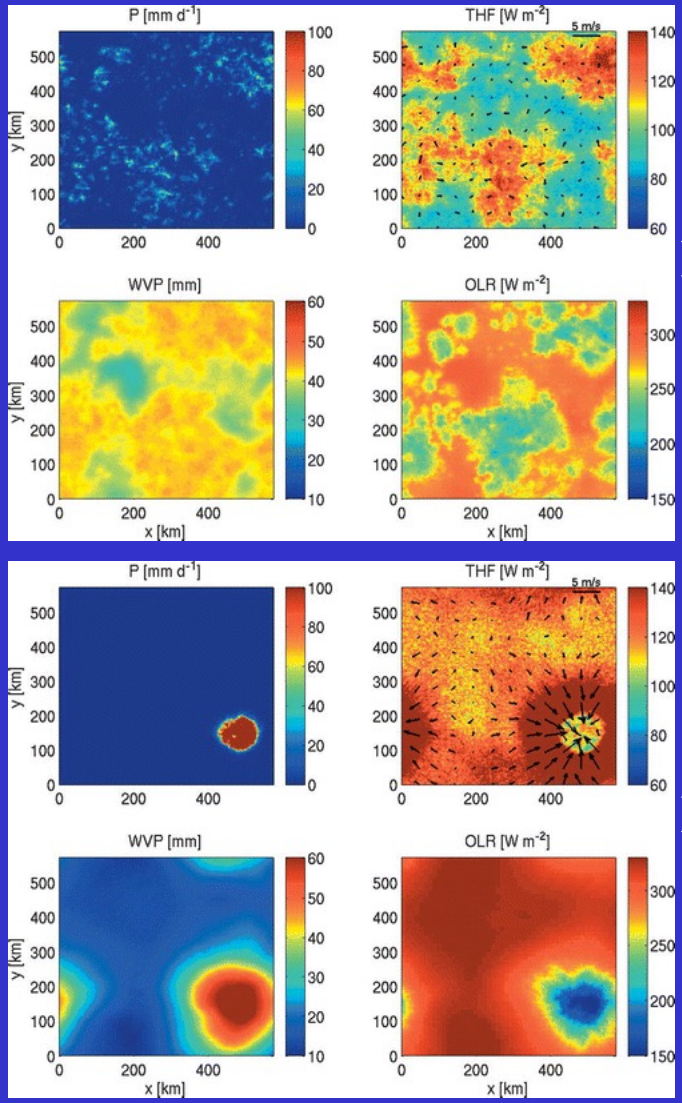

Bretherton *et al.* (2005)

What is convective self-aggregation (CSA)? Conventional Global Climate Model (GCM) examples

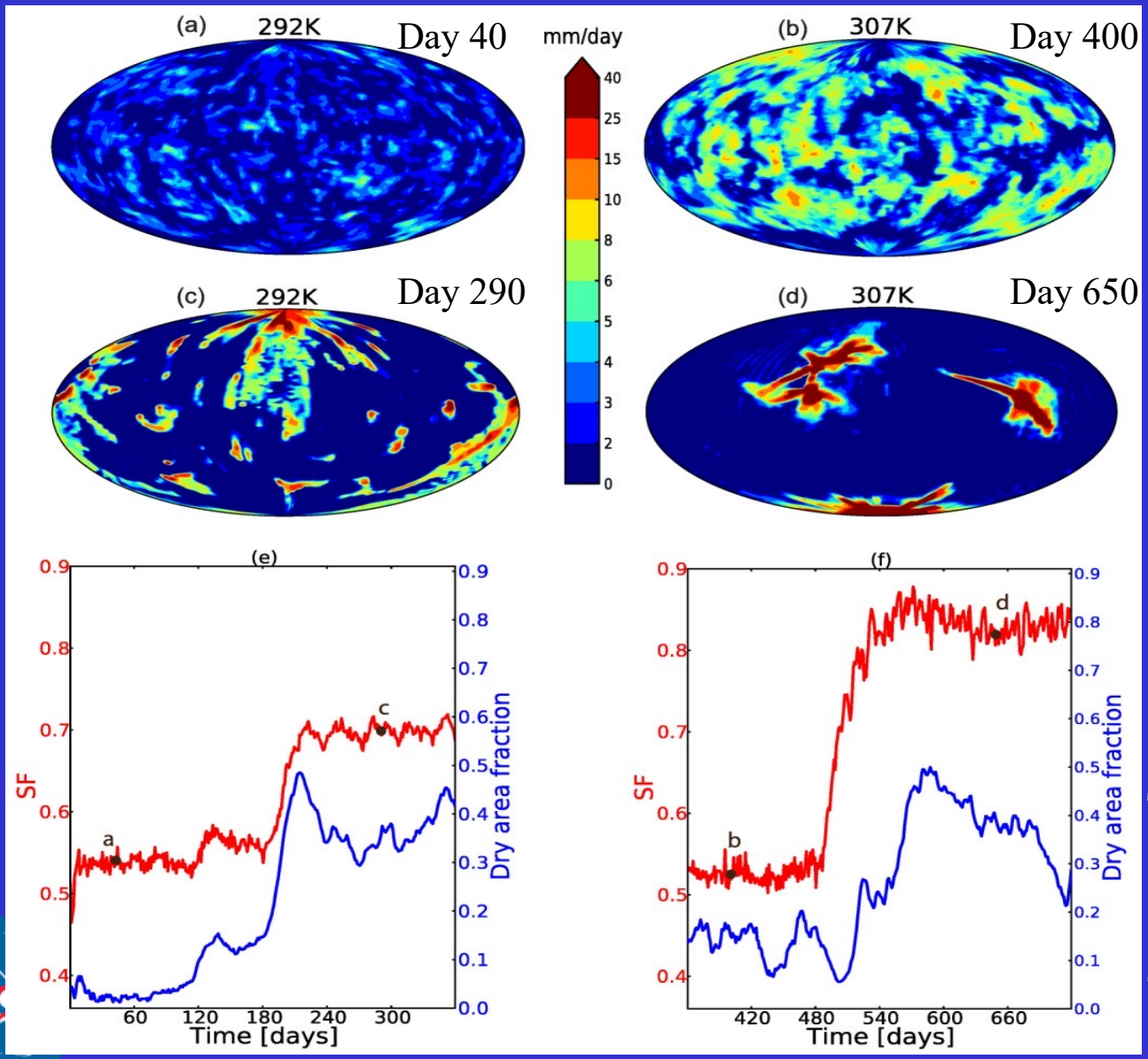

Take longer time to self-aggregate in GCM

Coppin & Bony (2015)

Relevance of CSA to observed convective organization

How relevant is self-aggregation physics to real-world convective organization?

–Radiative-convective equilibrium over small domains are rarely observed (Jakob *et al.,* 2019), whereas observed convective aggregation occurs at much larger spatial scales;

–SSTs are not uniformly distributed over large domains, where radiative-convective equilibrium is simulated with uniform SST by GCMs, MMF, and global CRMs;

–In reality, convective aggregation can occur under a variety of external forcings and spatial scales (Mapes, 1993; Nakazawa, 1988; Zeng, 2023);

–Observational analyses (Tobin *et al.,* 2012, 2013; Stein *et al.,* 2017) had to put restrictions on external forcings (factors) to infer some relationships of atmospheric variables (e.g., LW, SW, CWV) with the degree of convective aggregation;

–What convective aggregation index should be used? For example, the number of clouds (*N*)? Simple convective aggregation index (SCAI; Tobin *et al.,* 2012)? Others?

Figures from Tobin *et al.* (2013)

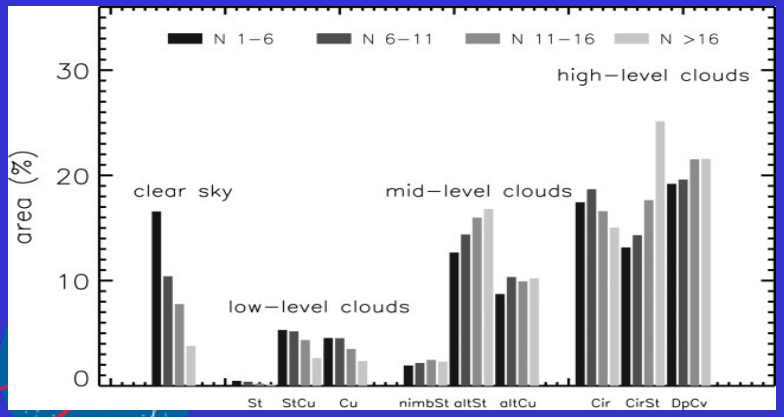

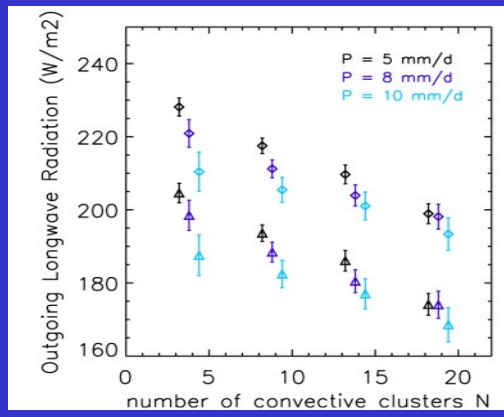

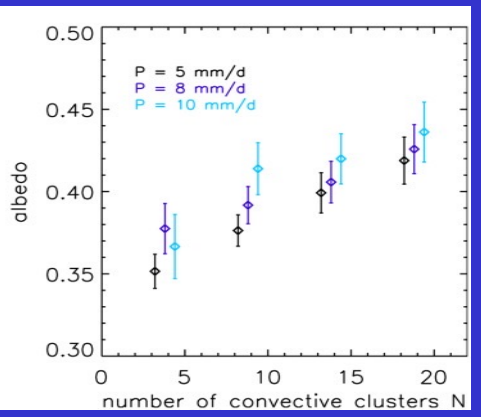

Objectives and methodology

Objectives

To provide an observational understanding of tropical convective aggregation,

- Particularly, the sensitivity of cloud properties and radiative fluxes by cloud type (p_c- τ) to the degree of convective aggregation at the 1000-km scale
- Intercomparison of convective aggregation indices and associated changes of cloud properties and radiative fluxes with the degree of convective aggregation

Data sets

1) CERES Single Scanner Footprint (SSF; 20 km x 20 km spacing): generate cloud objects, whose characteristics are used to calculate the degrees of convective aggregation
2) CERES Flux by cloud type (FBCT; 2 km x 2 km spacing): provide cloud properties and radiative fluxes by cloud type with seven p_c bins and six τ bins
3) MERRA-2: provide matched meteorological states, precipitation and ω_{500}

Analysis procedures

1) Oceanic (10°x10°) grids (46,220) only; also removed grids with strong ascents and weakest precipitation quintile (30,952 remaining grids)
2) Analyze grids with the four remaining precipitation quintiles
3) Compare the differences between strong and weak aggregation subpopulations according to aggregation indices (*N,* SCAI, MCAI and COP to be described later)

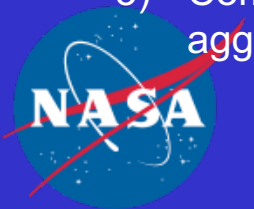

Mean p_c- τ distribution of single vs. multiple object grids

Single

Multiple

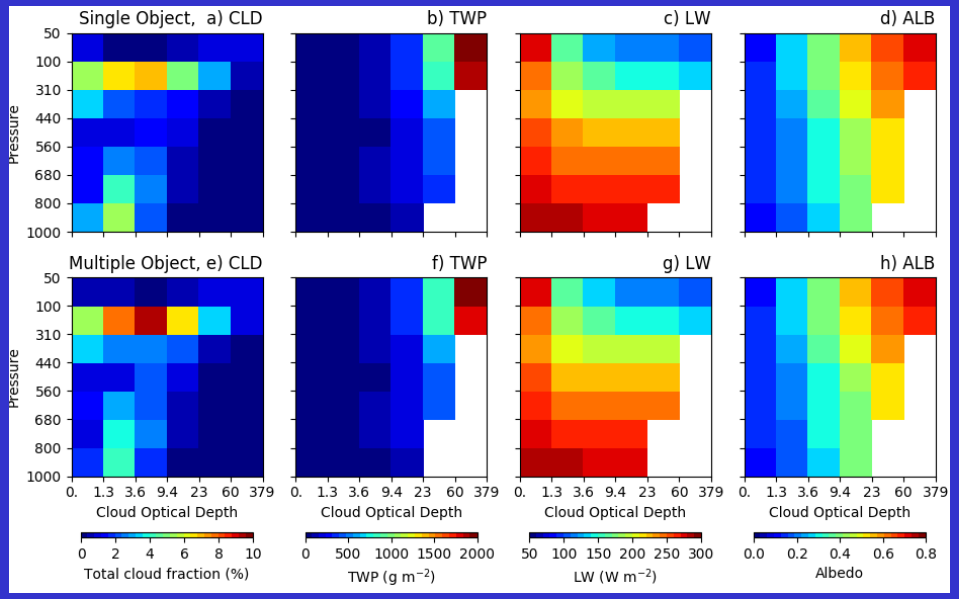

Single

Multiple

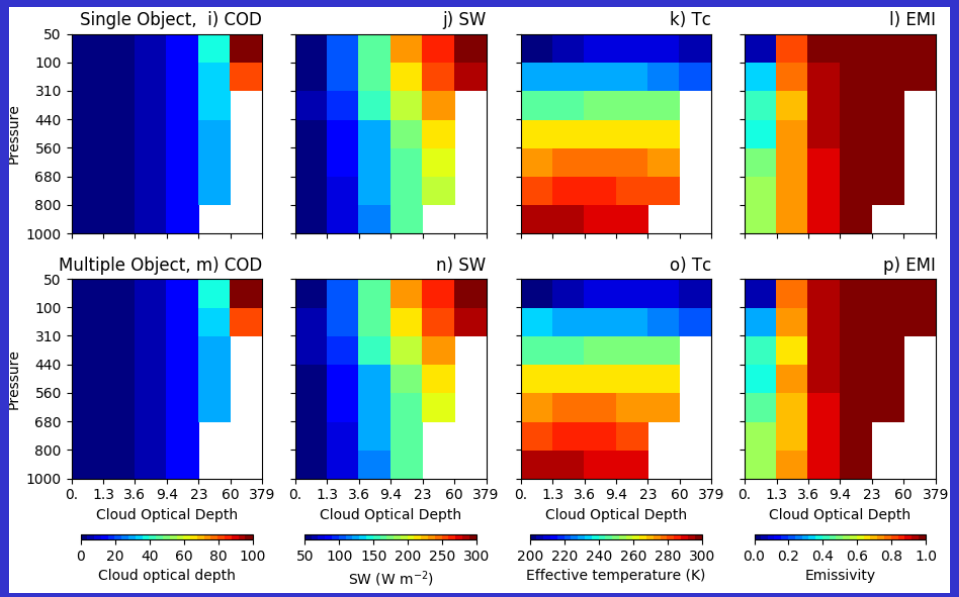

1. All cloud properties and radiative fluxes are similar between the single- and multi-object subsets, with the exception of cloud area fraction
2. Multi-object object subset has more upper-level clouds but fewer low-level clouds

Dividing data into five precipitation (quintiles) regimes

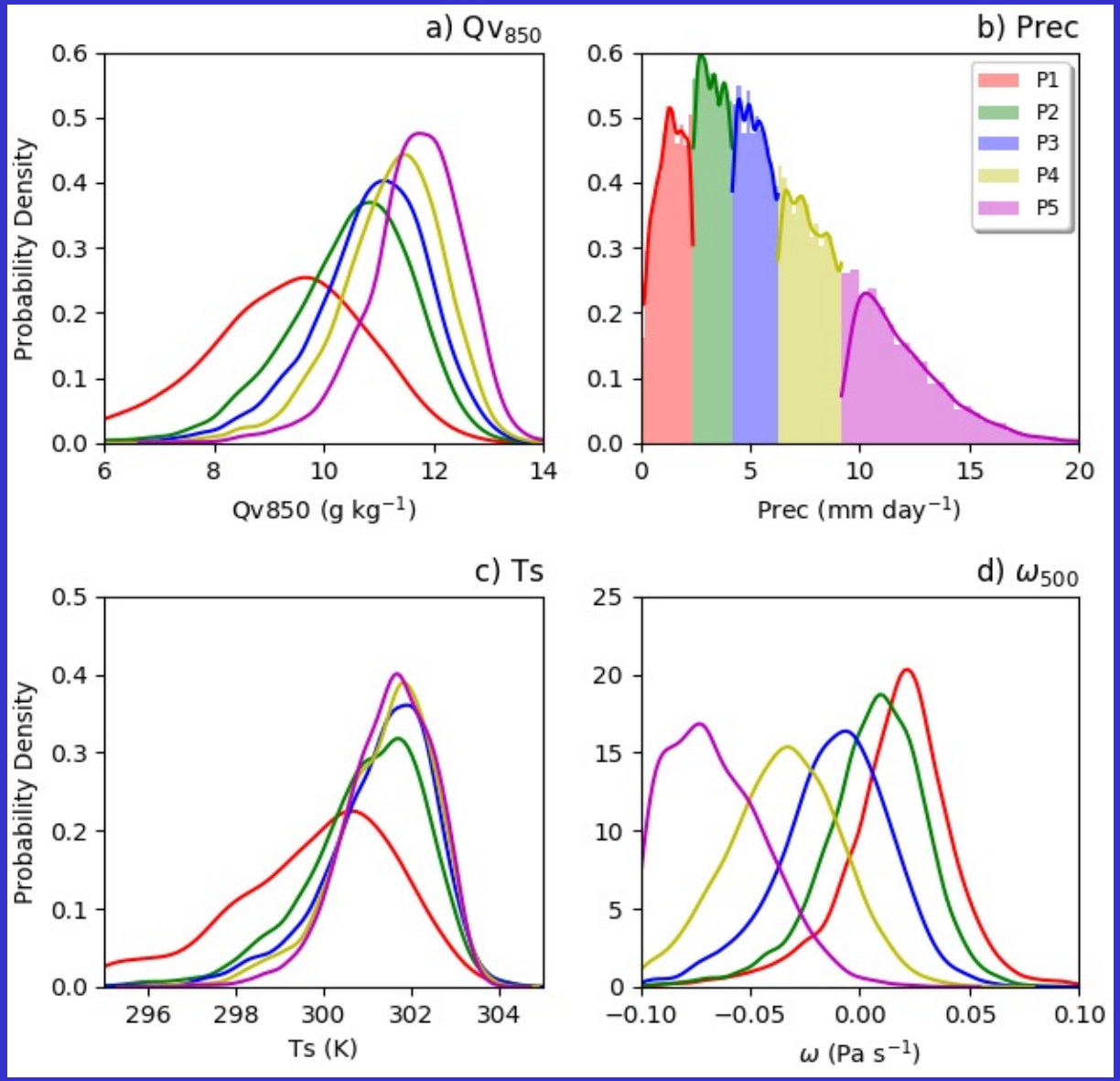

First quintile stands out: grid-averaged subsidence, lower SST and lower humidity.
Both the large-scale ascent and moisture increase with precipitation increase.

Cloud area fraction deviation (from the entire data set) dependency on *N* (1, 2, 3 & 4+) for P2 and P4 regimes

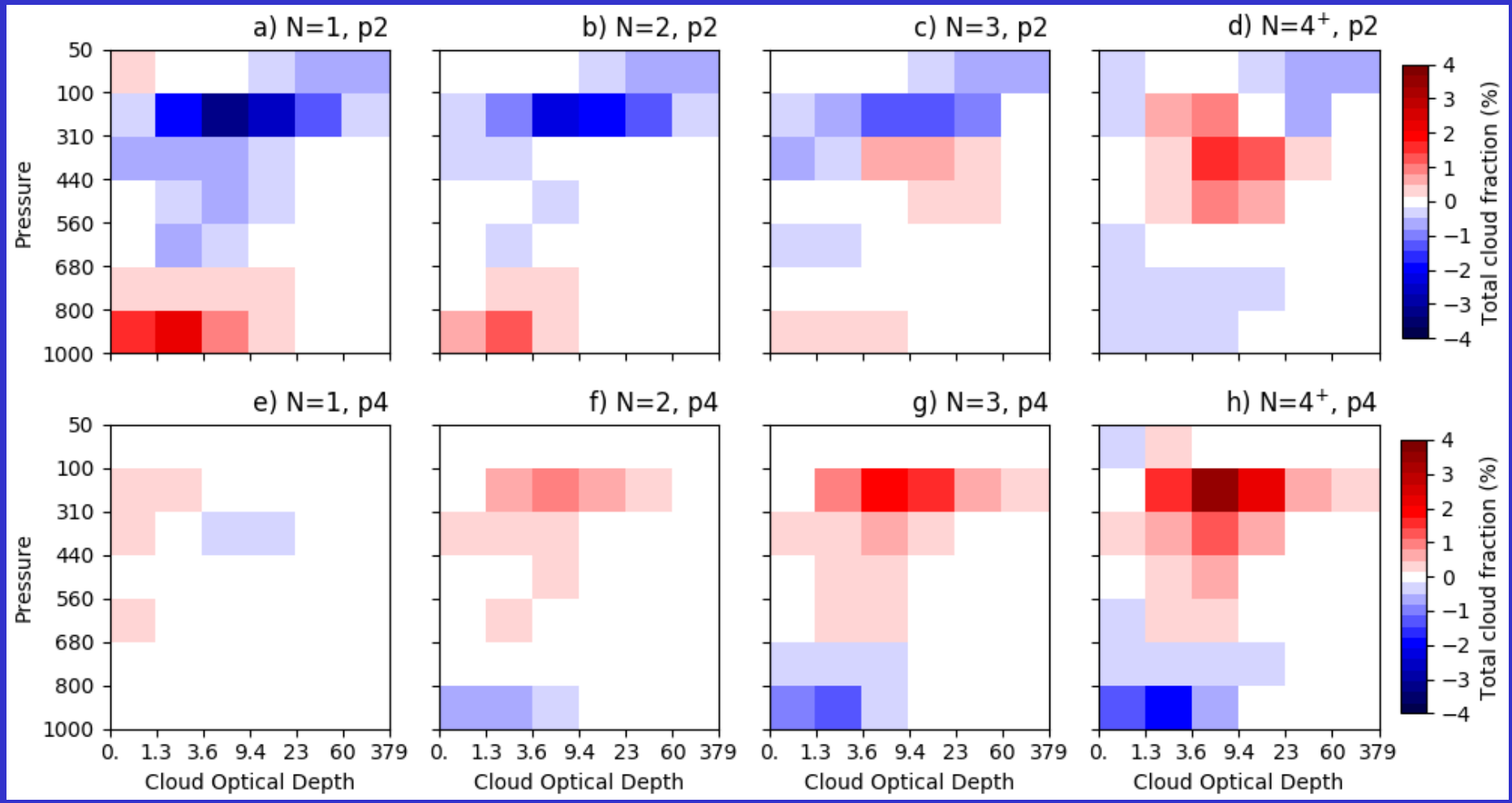

1. Both middle- and upper-level (anvil) clouds increase as *N* increases;
2. Low-level clouds decrease as *N* increases;
3. Differences between the two precipitation regimes are very pronounced, which are associated with different large-scale dynamics (e.g., ascent magnitudes).

Compare with Tobin *et al.* (2013) results

1. Tobin *et al.* identified cloud clusters with Meteosat-5 5-km (at nadir) Tb data;
2. Cloud objects are identified from 20-km (at nadir) SSF data;
3. Cloud area fractions are from ISCCP 30-km DX data in Tobin *et al.*, but 2-km FBCT data.

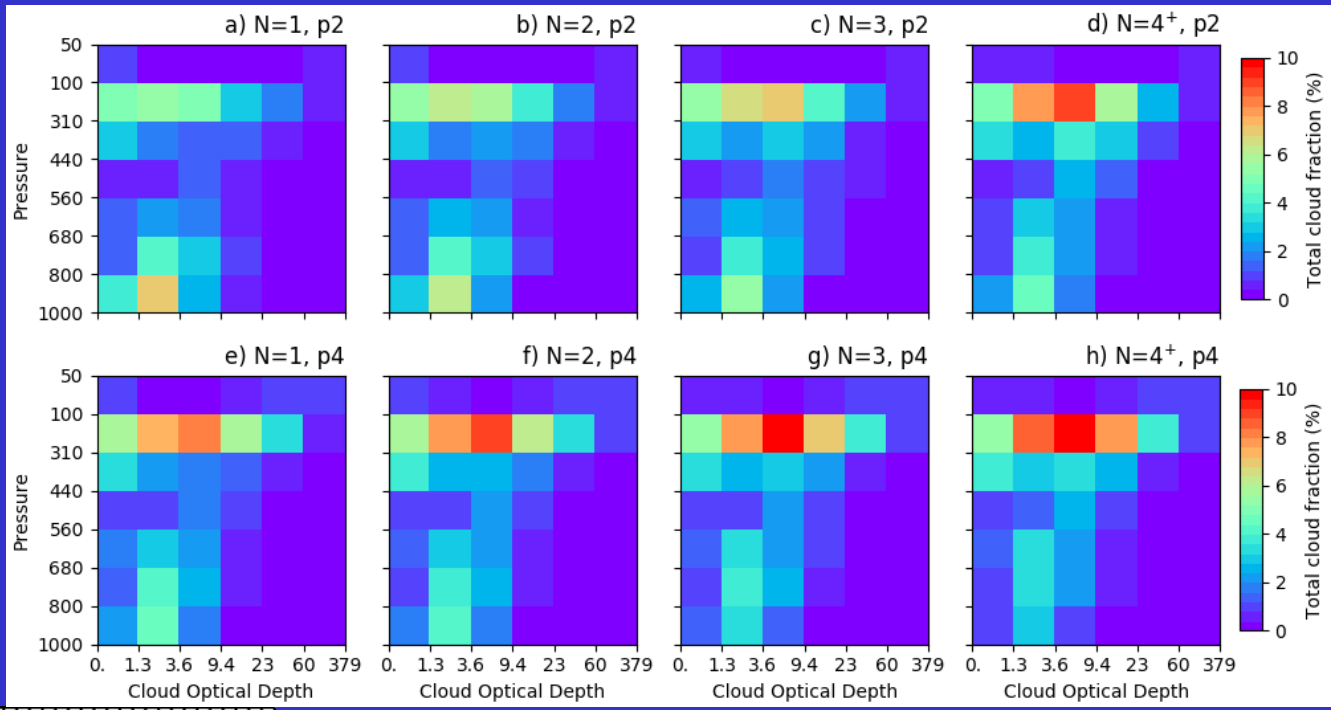

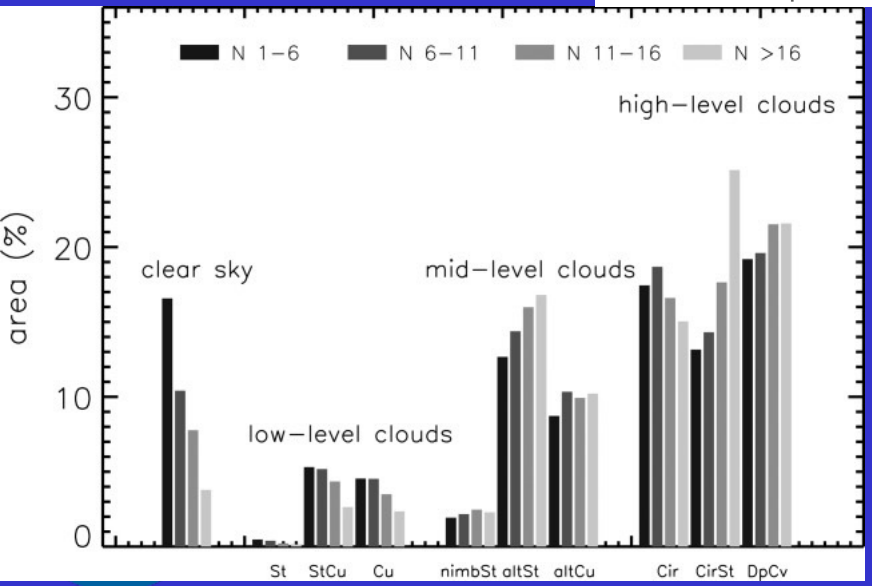

1. Consistent trends for clear sky (34.9 → 23.8% for P2; 24.4 → 18.2% for P4), low, middle and high cloud types except for cirrus as *N* increases;
2. Different magnitudes of cloud area fraction for low-cloud types, cumulus vs. stratocumulus; middle-cloud types, altocumulus vs. altostratus vs. nimbostratus; and high-cloud types, deep convection vs. cirrostratus vs. cirrus.

Cloud area fraction differences between N = 1 and N = 3 and between N = 2 and N = 4^+ for P2, P3, P4 and All P

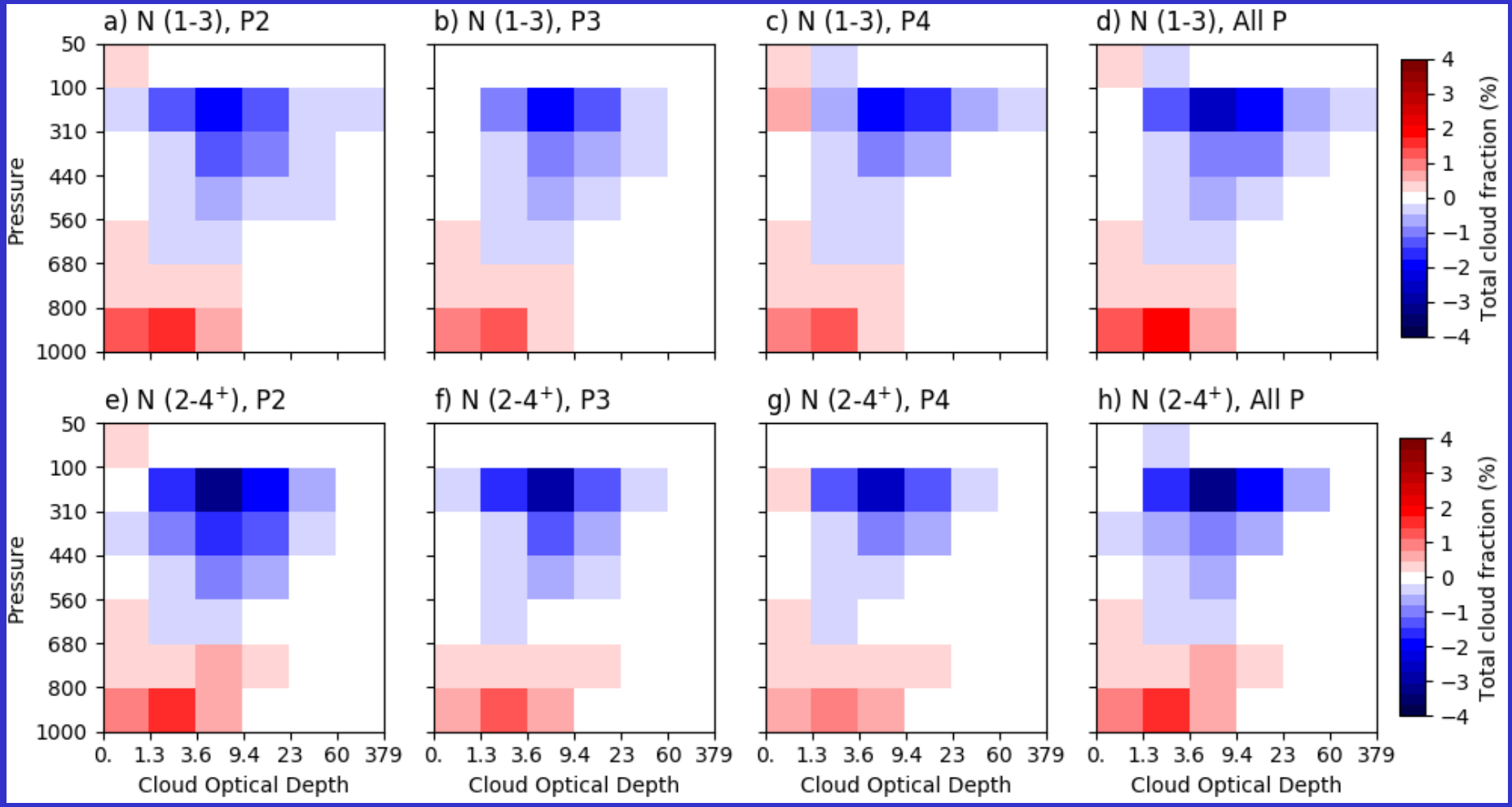

1. Despite of significant differences among *N*'s, cloud fraction differences between two *N subsets* are small among the different precipitation regimes;
2. This result suggests that *N* may be a good measure of convective aggregation (Tobin *et al.*, 2012, 2013) to examine differences between two aggregation states;
3. No need for examining individual precipitation regimes because all P's are similar.

LW and albedo differences between N = 2 and N = 4^{+} for P2, P3, P4 and All P

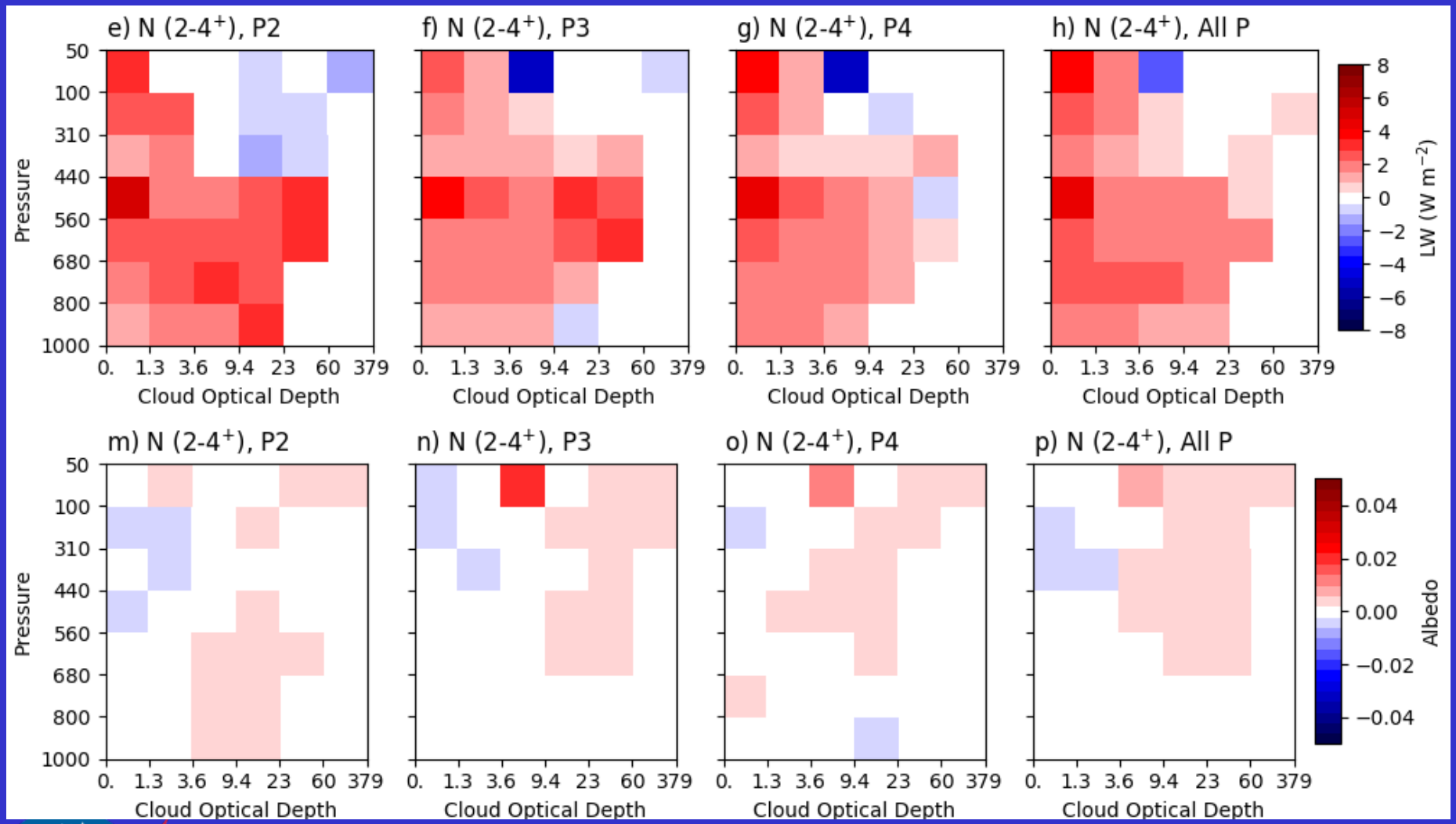

1. More infrared radiation is emitted to space (2-8 W m^{-2}) from optically-thin cloud types;
2. More solar radiation is reflected (2-4 W m^{-2}) from optically-thick cloud types.

Grid-mean SW and LW changes between N = 2 and N = 4$^+$ for P2, P3, P4 and All P

$$\Delta\bar{F} = \Delta a\,(F_c - F_e) + a\,\Delta F_c + (1-a)\,\Delta F_e$$

a is the cloud area fraction; subscripts *c* and *e* denote cloudy and clear sky, respectively
The first term represents the cloud radiative effect resulted from change in cloud area fraction
The 2nd and 3rd terms represent radiative flux changes in the cloudy and clear sky, respectively

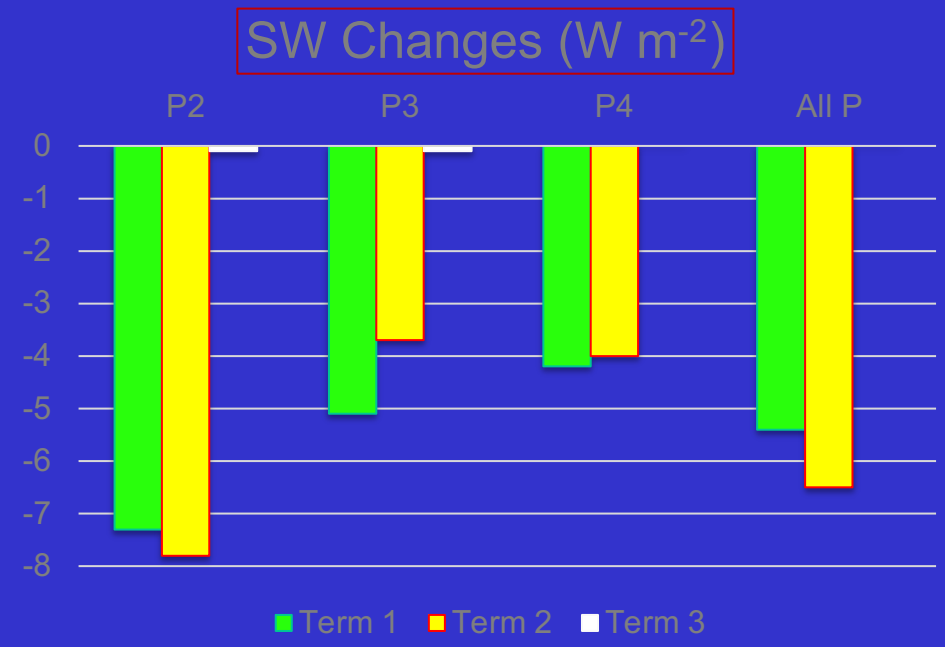

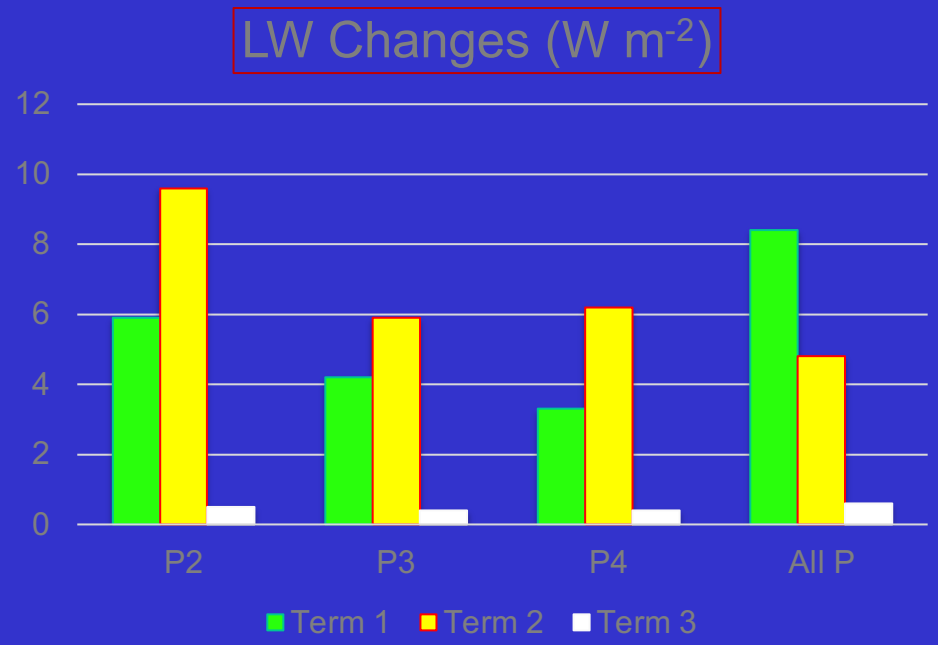

1. Changes in clear-sky area contribute greatly to the changes in both SW and LW, consistent with results obtained from grid-mean data (Tobin *et al.,* 2013);
2. Changes in cloudy-sky fluxes are equally or more important, particularly for LW;
3. There are very small changes in the clear sky.

Definition of convective aggregation indices

- Simple Convective Aggregation Index (SCAI) (Tobin *et al.* 2012)
- $SCAI = \frac{N}{N_{max}} \frac{D_0}{L} \times 1000$
- *N*: number of cloud objects; *L* domain lengthscale
- N_{max}: maximum of cloud objects within a domain
- D_0 is the geometrical mean of distances ($d_{i,j}$) between objects; $D_0 = \sum_{i=1}^{N} \sum_{j=i+1}^{N} d_{i,j} \Big/ \frac{1}{2} N(N-1)$

- A modification to SCAI (MCAI) (Xu *et al.*, 2019)
- Reduce the distances ($d_{i,j}$) between centroids of two objects by the sum of their radii
- $d'_{i,j} = d_{i,j} - (\sqrt{A_i} + \sqrt{A_j})/\sqrt{\pi}$
- MCAI → 0 if $D_0(d'_{i,j}) \rightarrow 0$, but SCAI does not → 0 as $D_0(d'_{i,j}) \rightarrow 0$
- MCAI = 0 (maximum aggregation)

- Convective Organization Potential (COP) (White *et al.* 2018)
- Interaction potential: $V(i,j) = \frac{\sqrt{A_i} + \sqrt{A_j}}{d(i,j)\sqrt{\pi}}$
- $COP = \sum_{i=1}^{N} \sum_{j=i+1}^{N} V(i,j) \Big/ \frac{1}{2} N(N-1)$
- A_i, A_j are areas of *i*th and *j*th objects, respectively

$0 \leq COP \leq 1$ (maximum aggregation)

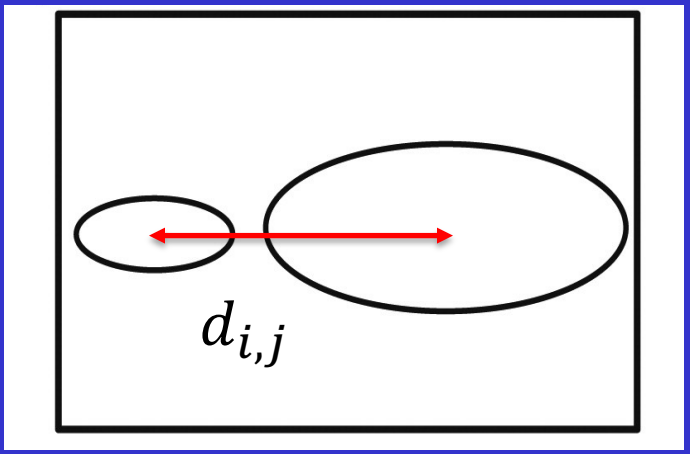

Comparison of Weak, Moderate and Strong Aggregation Terciles of SCAI, MCAI and COP

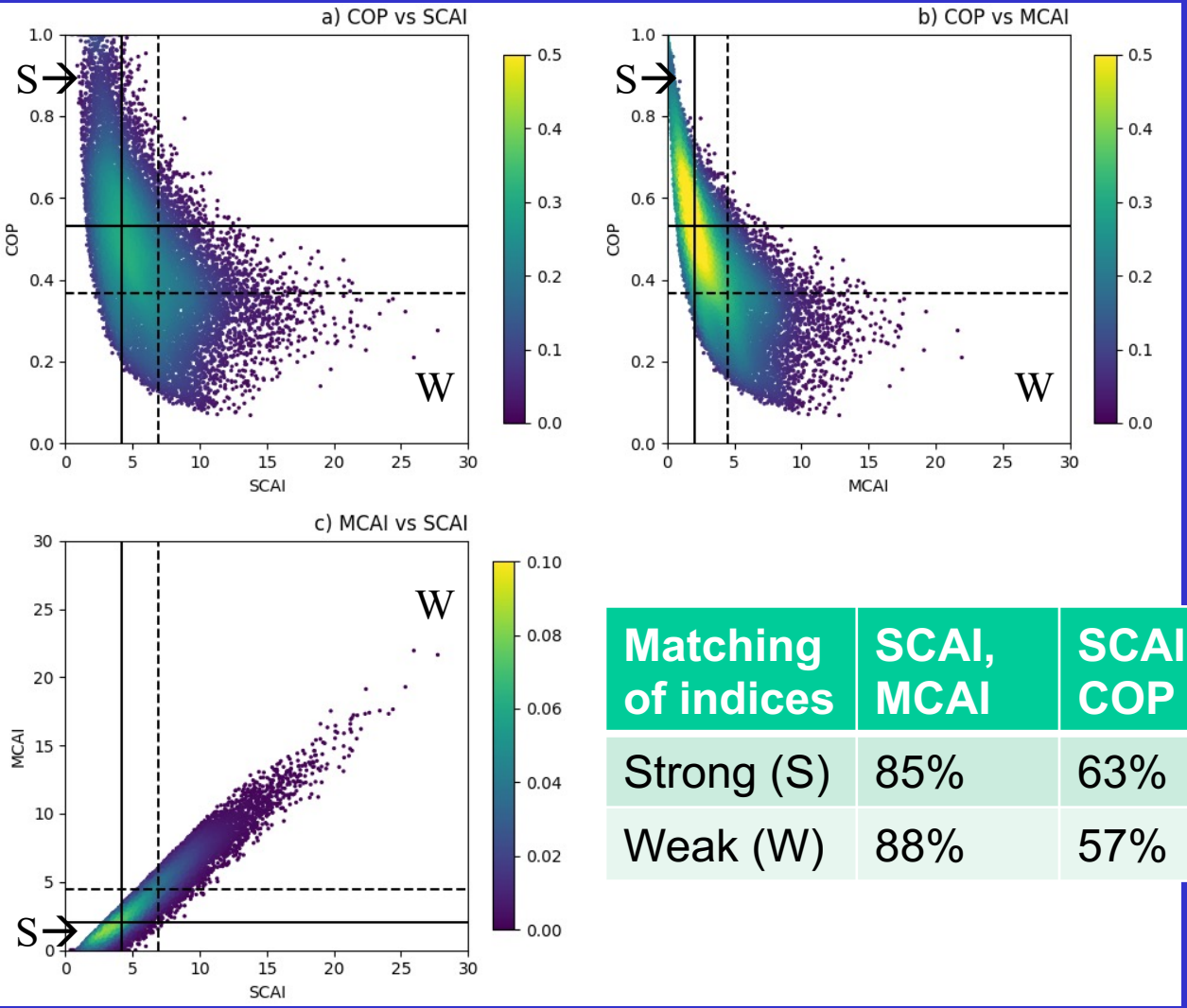

Matching of indices	SCAI, MCAI	SCAI, COP	MCAI, COP
Strong (S)	85%	63%	78%
Weak (W)	88%	57%	68%

SCAI and MCAI are much closely matched (>85%), compared to that between SCAI and COP (~60%);
Strong terciles are better matched by 10% than weak terciles between MCAI and COP.

Cloud fraction difference and its relative change (RC) between strong and weak aggregation terciles of SCAI, MCAI and COP

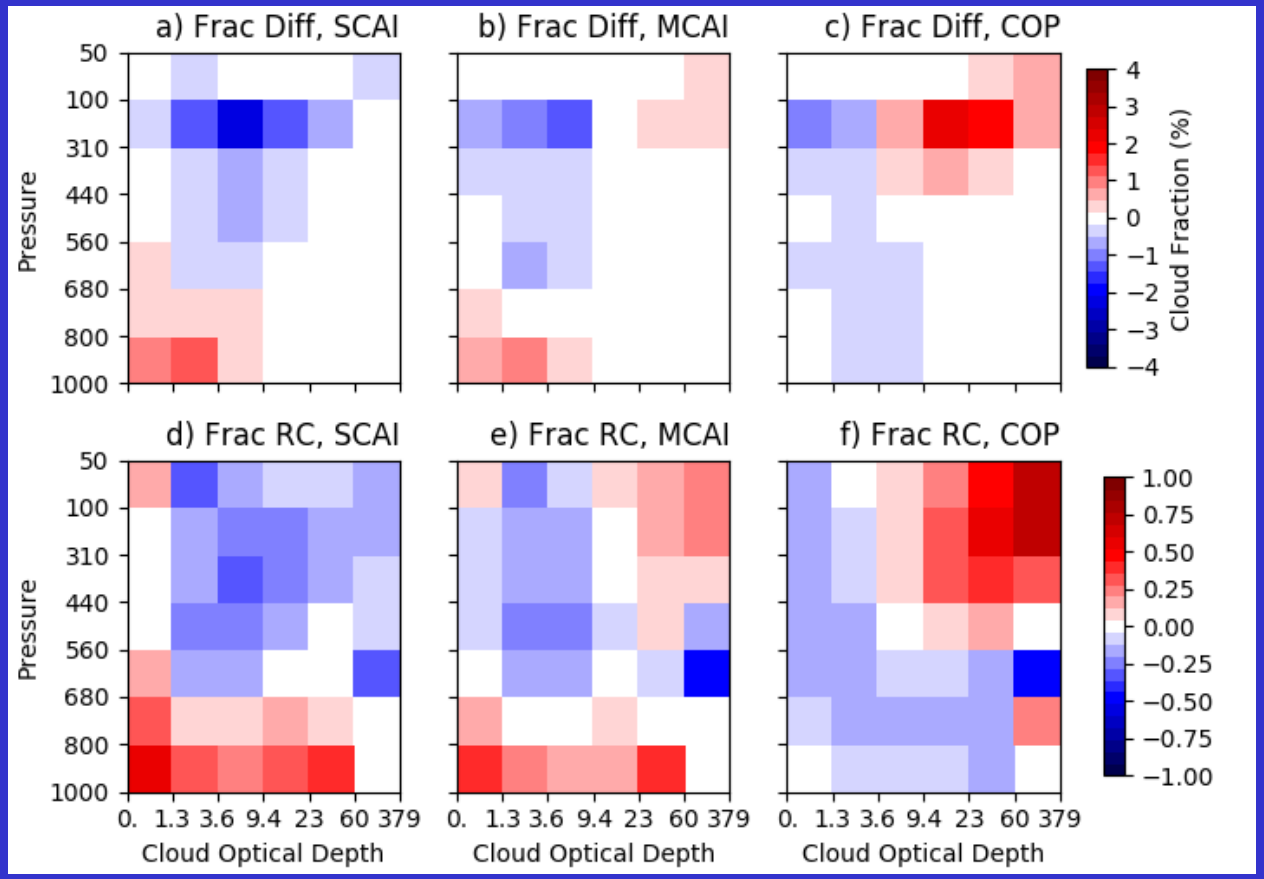

1. The cloud area fraction difference using SCAI is similar to that using *N* as an index;
2. Using COP, area fractions of optically-thick high-level cloud types increase, but those of low-level cloud types decrease; with MCAI between SCAI and COP;
3. There are large relative changes for low-level (SCAI and MCA) and optically-thick upper-level (COP) cloud types.

LW, SW and albedo differences between strong and weak terciles

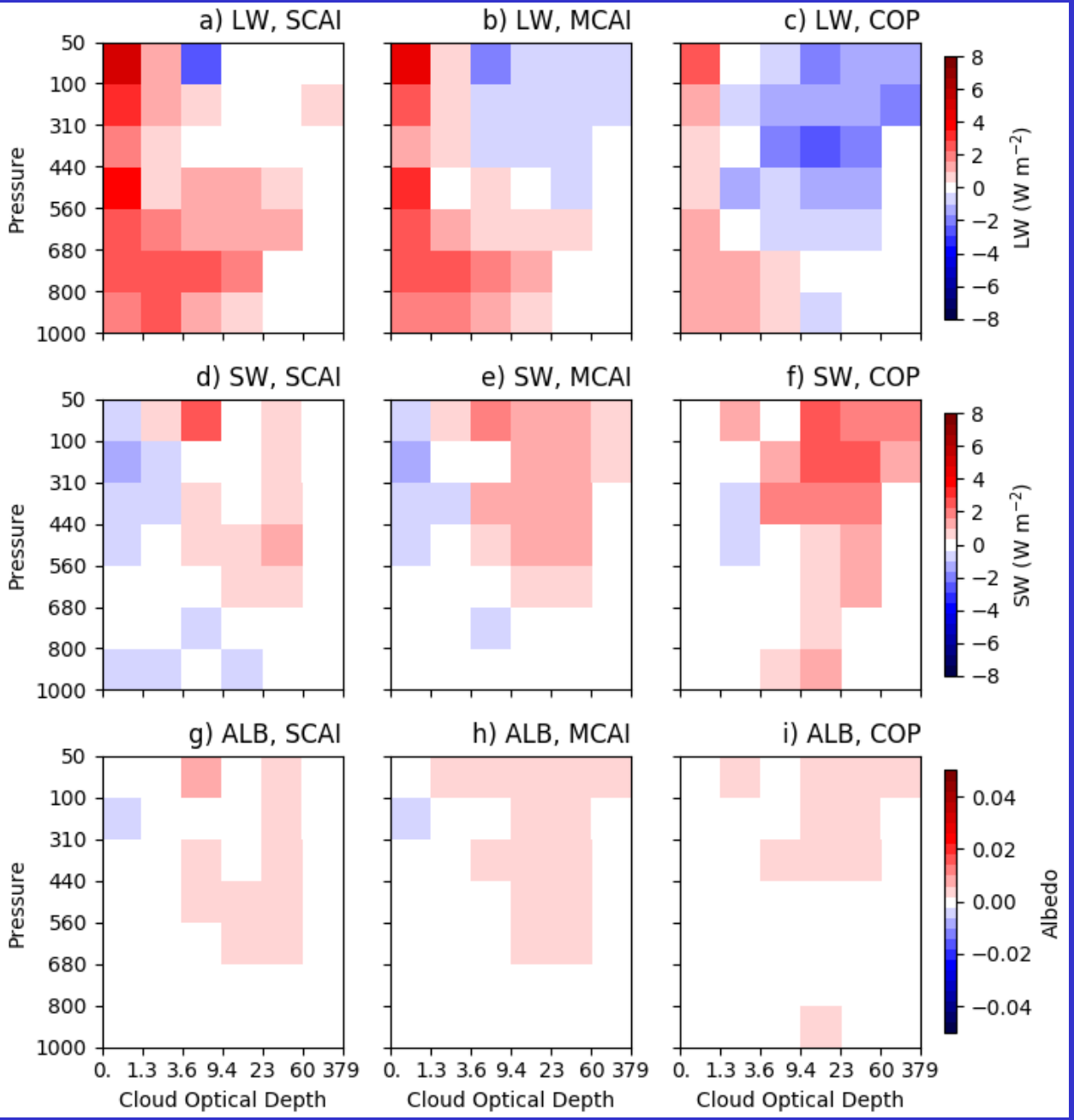

Cloud area fraction difference between strong and weak aggregation terciles of SCAI, MCAI and COP

How to explain the differences for the deep convective cloud types?

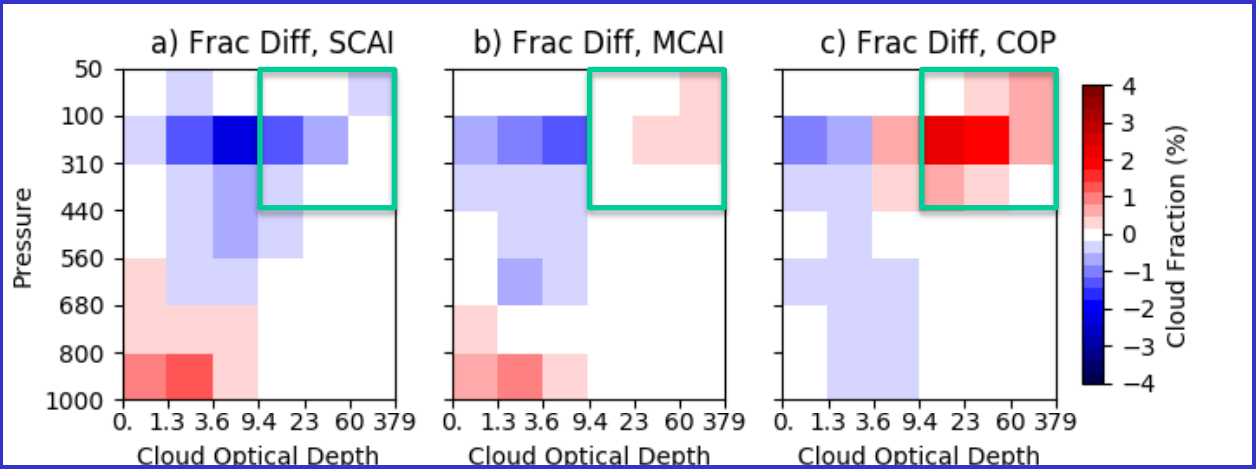

Partitioning and weighted cloud-object footprint numbers (deep convective cloud types) of N=2, N=3 and N=4+ grids in strong and weak terciles of SCAI, MCAI & COP

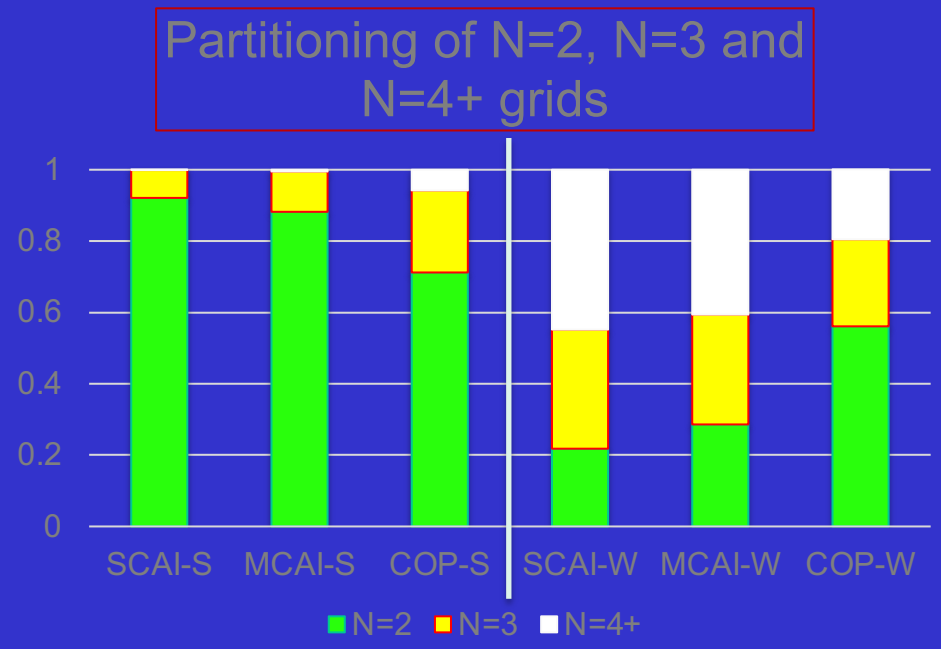

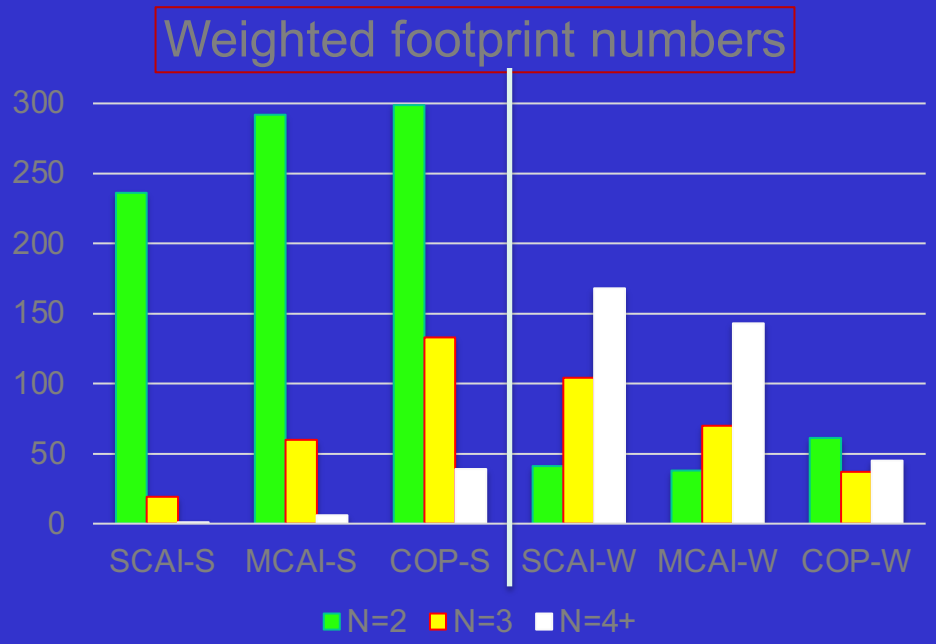

1. The dominance of N=2 in the strong terciles is weakened from SCAI, MCAI to COP; The trend in the weak terciles is similar for N=3 and 4+, but opposite for N=2;
2. The contribution of optically-thick upper-level clouds increases from SCAI, MCAI to COP in the strong terciles, but decreases in the weak terciles (except for N=2).

Summary

1) Changes of cloud properties and radiative fluxes with SCAI are similar to those with N as an index, agreeing with prior studies using grid-mean properties.
2) For changes from weak to strong degrees of aggregation using N and SCAI,
   - area fractions of middle- and high-level cloud types decrease by up to 4% but those of low-level cloud types increase by up to 2%,
   - more infrared radiation is emitted to space (2-8 W m^{-2}) from optically thin cloud types,
   - more solar radiation is reflected (2-4 W m^{-2}) from optically-thick cloud types.
3) However, using COP (MCAI to lesser extent),
   - area fractions of optically-thick cloud types increase; these cloud types emit less infrared radiation and reflect more solar radiation,
   - area fractions of low-level clouds decrease,
   - the different behaviors can be explained by greater expansion of cloud object sizes for COP than MCAI/SCAI as the degree of convective aggregation increases.
4) Cloud radiative effects due to changes in clear-sky area contribute greatly to the changes in both the grid-mean SW and LW fluxes, and so are changes in cloudy-sky fluxes, particularly for LW.

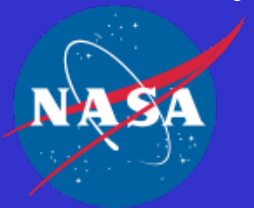

Selection of convective cloud objects

(Xu *et al.* 2005, 2007, 2008, 2016, 2017)

- A contiguous patch of cloudy regions with a single dominant cloud-system type; no mixture of different cloud-system types
- The shape and size of a cloud object is determined by
  - the satellite footprint data
  - the footprint selection criteria
- Selection criteria for deep convective cloud objects:
  - cloud optical thickness $\tau > 10$, and
  - cloud top height $z_{top} > 10$ km, and
  - overcast